Growth of Noncircular and Faceted Holes in Liquid–Liquid Dewetting of Thin Polymer Bilayers

ARTICLE *in* MACROMOLECULES · DECEMBER 2011

Impact Factor: 5.8 · DOI: 10.1021/ma201538p

3 AUTHORS, INCLUDING:

Lin Xu
University of Minho
15 PUBLICATIONS **136** CITATIONS
SEE PROFILE

Ashutosh Sharma IITK
Indian Institute of Technology Kanpur
335 PUBLICATIONS **7,410** CITATIONS
SEE PROFILE

Macromolecules

ARTICLE

pubs.acs.org/Macromolecules

Growth of Noncircular and Faceted Holes in Liquid−Liquid Dewetting of Thin Polymer Bilayers

Lin Xu,[†] Ashutosh Sharma,*[,†,‡] and Sang W. Joo*[,†]

[†]School of Mechanical Engineering, Yeungnam University, Gyongsan 712-749, South Korea

[‡]Department of Chemical Engineering, Indian Institute of Technology, Kanpur 208016, India

ABSTRACT: Although the formation of circular holes is the norm in the spontaneous dewetting of thin polymer films, we show highly anisotropic hole growth leading to irregular and faceted shapes in dewetting of the upper polystyrene layer in a thin polymer bilayer (silica−PMMA−PS−air). The irregular shapes are formed when viscous dissipation is dominated by the upper PS dewetting layer under the conditions of its much higher viscosity and lower thickness or the lower viscosity and higher thickness of the substrate PMMA layer. These conditions engender strong slippage of the dewetting layer, resulting in very broad rims and the long-range viscous interactions among randomly distributed, initially circular holes. The growth occurs selectively in the directions of less viscous resistance. Thus, the irregular growth of holes can be inhibited by increasing the PS film thickness or by decreasing the PMMA film thickness.

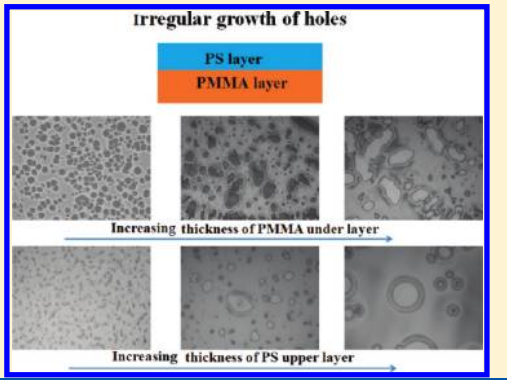

INTRODUCTION

Thin polymer films are found in a host of modern technologies from coating, painting, lithographies, self-organized patterning, diffusion, to multilayer adsorption, etc. Instability of thin polymer films on a solid substrate is thus an important phenomenon. The usual scenario for the initial stages of dewetting of a thin (<100 nm) film on a solid substrate with no slip involves the formation and growth of nearly circular holes.[1−6] The polymer mass from the dewetted regions is collected in a narrow elevated rim of at the perimeter of the holes, which in some cases may show periodic undulations owing to the cross-sectional curvature. A gross distortion of the circular shape to form faceted sides occurs only in the later stages when the rims of the neighboring holes overlap and the repeated hole mergers result in a polygonal structure. Eventually, the edges of polygons can decay into droplets. The many structural and mechanistic aspects of the formation and growth of holes on a solid substrate are now reasonably well understood.[7−12] However, the dewetting of a thin polymer film on liquid substrate is a far richer phenomenon because the liquid−liquid interface, unlike the liquid−solid interface, can deform in the dewetting process.[13−33] In the liquid−liquid dewetting process, the morphology of the liquid−liquid interface can self-adjust to optimize the dewetting velocity. Previous studies[13−33] have reported that the film thickness and the molecular weight of the underlayer can strongly influence the deformation of liquid−liquid interface and the dewetting kinetics. Experiments of Lambooy et al.[14] have reported the influence of the molecular weight of the PMMA lower layer on the dewetting velocity of the PS upper layer. Recently, simulations of Merabia et al.[25] have revealed that the viscosity ratio between the upper layer and the underlayer can also influence the dewetting kinetics by controlling the mechanisms of viscous dissipation in the liquid−liquid dewetting. Although nearly circular holes are witnessed in all of the experimental studies of bilayers, some recent simulations[32] point to the possibility of elongated holes under the conditions that favor strong slippage of the dewetting film on relatively thick underlayers of much lower viscosity. There is as yet no experimental study of the formation, growth, dynamics, and morphology of noncircular holes. Strong slippage in dewetting offers novel pathways for auto-optimization of dewetting by morphological changes that are not accessible when dewetting occurs under the conditions of no slip. For example, a slipping straight dewetting line forms spatially periodic undulations that elongate into long fingers that continuously disintegrate into droplets that are left behind.[34] This mechanism regulates the dewetted mass collected in the rim (and its width) to a constant low value, thus decreasing the viscous dissipation in the rim and an autoregulation of the contact-line velocity to a constant high value. In the absence of fragmenting fingers, the velocity of dewetting in a strongly slipping film should decline with time as $V \sim t^{-1/3}$ because of a continuous buildup of a rim.[34]

Here, we explore the morphology of growing holes in liquid−liquid dewetting of an unstable upper PS layer on a PMMA film in a thin polymeric bilayer system (silica−PMMA−PS−air). In particular, we focus on the conditions that engender strong slip of the dewetting upper layer on the lower polymer layer. We thus show a new mechanism for the auto-optimization of dewetting by highly anisotopic growth of initially circular holes, leading to the formation of irregular and faceted dewetted regions. A bilayer offers the possibility of readily altering the extent of effective slippage felt by the upper layer by changing the

Received: July 6, 2011
Revised: October 4, 2011
Published: November 09, 2011

relative viscosities and thicknesses of the two layers. Previous studies[15−18] on bilayers have shown nearly isotropic growth of circular holes. However, the conditions explored have not allowed for the possibility of strong slippage which, as shown here, happens when the viscosity of a relatively thick substrate layer is several orders smaller than that of the dewetting layer. When the relative viscous resistance offered by the substrate layer becomes low, the liquid−liquid interface becomes highly mobile, approaching the condition of a shear free interface or infinite slip. In this case, the mechanism of energy loss becomes different from the dewetting on the solid substrate and on the more viscous liquid substrates.[25] In the latter case of dewetting with no slip, the viscous dissipation is highly localized near the contact line, whereas it is distributed over the entire broad rim of a low height in the case of strong slip.[34−38] This rather even distribution of the dewetted mass in the intervening film between the holes[36−38] is because of a negligible viscous resistance allowing a fast distribution of fluid at greater distances from the growing holes. This is unlike the case of nonslipping[6,39] and weakly slipping films[36−38] where sharply rising, narrow rims form around holes because higher flow resistance makes the escape of liquid from the rim very slow. Owing to their broad rims, the viscous interactions between the two neighboring holes acquire a long-range correlation.[36−38] This should allow some interesting, nontrivial possibilities for self-organization by anisotropic growth of holes in the directions of less resistance. Indeed, in the experiments reported here, it is found that the holes grow anisotropically into irregular and faceted shapes under the conditions of much lower viscous dissipation in the underlayer, e.g., when the viscosity (thickness) of the underlayer is much smaller (higher) than that of the upper layer and the upper layer polymer chains are entangled. In the dewetting process, we find elliptic-like holes, triangular and reactgular holes, and holes with other more irregular shapes.

EXPERIMENTAL SECTION

The system under investigation is a polymeric bilayer of polystyrene (PS2.4k-M_w = 2.4 kg/mol, PS4k-M_w = 4 kg/mol, PS48k-M_w = 48 kg/mol, PS390k-M_w = 390 kg/mol, and PS2000k-M_w = 2 000 kg/mol; M_w/M_n < 1.1) and poly(methyl methacrylate) (PMMA10k-M_w = 10 kg/mol, PMMA15k-M_w = 15 kg/mol, PMMA50k-M_w = 50 kg/mol, and PMMA350k-M_w = 350 kg/mol; M_w/M_n < 3) on the Si wafer with 120 nm oxide layer. PMMA films were first directly spin-coated from a chloroform solution onto the Si wafers. PS films were spin-coated from a toluene solution onto the mica wafers. The bilayer films were prepared by floating of the PS films on deionized water and then transferring them on the PMMA films. The thickness of the films was measured by ellipsometry. To initiate the dewetting process, the samples were heated to a temperature well above the glass transition temperature of PS in air. At the experimental temperature of 180 °C, the viscosities of PS2.4k, PS4k, PS48k, PS390k, PS2000k, PMMA10k, PMMA15k, PMMA50k, and PMMA350k are 0.103, 0.585, 2.72 × 10^3, 2.46 × 10^6, 4.99 × 10^8, 3.1 × 10^3, 1.23 × 10^4, 7.37 × 10^5, and 5.508 × 10^8 Pa·s, respectively.[40−42] The surface morphology was observed by optical microscopy (OM) in the reflection mode and atomic force microscopy (AFM) operating in the tapping mode. The spring constant of the AFM cantilever was 2 N/m. The cantilever was oscillated close to its resonance frequency between 65 and 75 kHz. The PS upper layer was removed by immersing the samples in a selective solvent—cyclohexane—in order to characterize the PMMA−PS interface during dewetting. The previous papers on the PMMA−PS bilayers[14,16−18] have also used cyclohexane for removal of PS because it does not influence the morphology of the remaining PMMA layer. After drying, the exposed PMMA surface was imaged to obtain the morphology of the PS/PMMA interface.

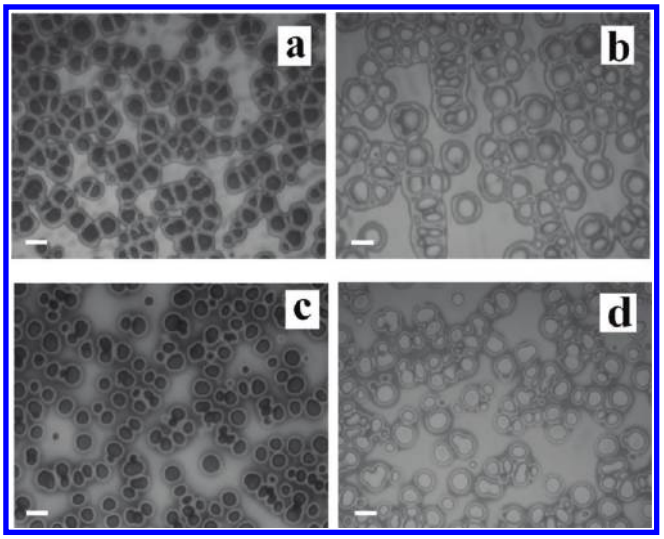

Figure 1. Optical micrographs of the morphology of the liquid−gas interface in nonslipping films at late stages of growth when the holes are in the process of coalescence. The PS (h_U = 55 ± 2 nm) film/the PMMA film (M_w = 15 kg/mol, different film thickness h_L)/the Si wafer with 120 nm oxide layer was heated at 180 °C. (a) PS: M_w = 48 kg/mol, h_L = 82 nm, annealing time is 40 s; (b) PS: M_w = 48 kg/mol, h_L = 236 nm, annealing time is 30 s; (c) PS: M_w = 390 kg/mol, h_L = 82 nm, annealing time is 150 s; (d) PS: M_w = 390 kg/mol, h_L = 236 nm, annealing time is 90 s. The size of the bar is 20 μm.

RESULTS AND DISCUSSION

A series of OM images in Figure 1 show the morphology of two PS films (M_w = 48 and 390 kg/mol, h_U = 55 ± 2 nm) on two different thickness PMMA layers (M_w = 15 kg/mol, h_L = 82 and 236 nm). For these samples, the viscosities of PS layer are 2.72 × 10^3 and 2.46 × 10^6 Pa·s, as compared to the PMMA underlayer viscosity of 1.23 × 10^4 Pa·s. From Figure 1, it is observed that for all of these systems (M_w = 48 and 390 kg/mol), the isolated holes grow isotropically in the early stages and the shape of the holes remains nearly circular until their narrow rims begin to overlap. Also, the film outside of the narrow localized rims continues to remain undisturbed and retains its uniform thickness. Basically, disturbance to the film heights are localized only in the immediate vicinity of a growing hole. As reported previously,[15−20] the holes in these bilayer systems eventually organize into polygonal structures that ultimately decay into stable droplets. We do not show the details of the late time process in these cases because it is similar to the previous observations on the formation of droplets. Thus, the anomalous growth of holes is not witnessed in dewetting on the liquid substrates that have viscosities higher than or even couple of orders lower than the viscosity of the dewetting layer and even when the lower layer thickness is much higher (<∼4* upper layer thickness). Apparently, a high degree of anisotropic hole growth requires much smaller viscous resistance in the underlayer, leading to a nearly shear-free interface and a substantial slippage, which is also aided by the chain entanglement in the upper dewetting layer. This can be achieved for example by increasing the molecular weight and viscosity of the upper layer greatly. In what follows, noncircular holes on a liquid substrate are discussed when the upper layer has far higher viscosity and the PMMA underlayer is made thicker, thus decreasing viscous dissipation in the substrate layer compared to in the dewetting layer. In all the cases of irregular

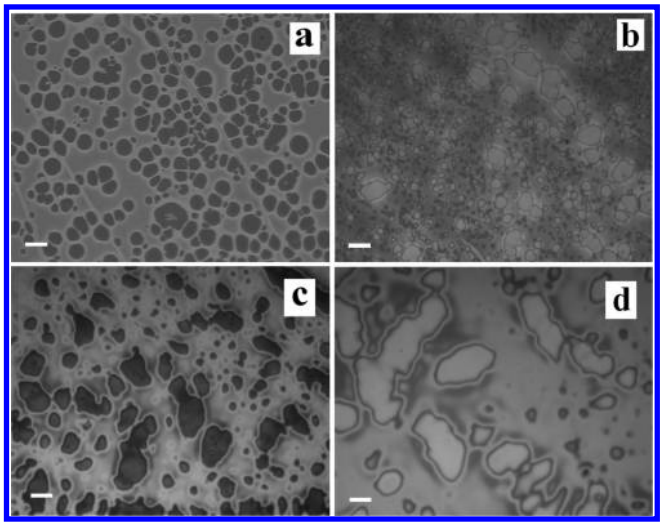

Figure 2. Optical micrographs show the morphology of the liquid−gas interface for increasing thickness of the substrate PMMA layer. The bilayer with PS (M_w = 2000 kg/mol, h_U = 42 ± 2 nm) film/the PMMA film (different film thickness h_L) was annealed at 180 °C. (a) PMMA: M_w = 15 kg/mol, h_L = 25 nm, annealing time is 140 min; (c) PMMA: M_w = 15 kg/mol, h_L = 48 nm, annealing time is 20 min; (c) PMMA: M_w = 15 kg/mol, h_L = 96 nm, annealing time is 20 min; (d) PMMA: M_w = 15 kg/mol, h_L = 262 nm, annealing time is 15 min. The size of the bar is 20 μm.

hole growth, the upper layer polymer chains are beyond the entanglement limit.

Figure 2 shows the morphology of a highly viscous PS film (M_w = 2000 kg/mol, h_U = 42 nm) on several PMMA (M_w = 15 kg/mol) layers of increasing thickness from 25 to 262 nm. When the PMMA underlayer is thin (h_L = 25 nm), the holes growth remains isotropic and the holes largely retain their circular shapes until the overlap of the neighboring hole rims. With the increase in the film thickness of the PMMA substrate layer to h_L = 48 nm, the growth and shape of the holes begin to become irregular. With a further increase in the PMMA underlayer thickness, the hole growth is clearly anisotropic and the holes no longer remain circular, but a variety of irregular shapes that become increasingly faceted with time are witnessed, as shown in the Figure 2c,d. Thus, a much higher viscosity of the dewetting PS layer coupled with a thicker substrate PMMA layer is able to decrease the viscous dissipation in the substrate layer vis-à-vis the PS layer sufficiently to engender noncircular growth of holes.

Figure 3 shows the time evolution of holes/dewetted regions in a selected case of irregular holes: the case of the high M_w PS film (M_w = 2000 kg/mol, h_U = 42 nm) on a low M_w, thick PMMA film (M_w = 15 kg/mol, h_L = 262 nm). Figure 3 clearly shows that on the thick PMMA underlayer anisotropic growth of dewetted regions results in noncircular holes that can acquire highly faceted shapes with lines and corners. Figure 3e depicts the dynamics of contact lines for noncircular holes that are encountered in our experiments. First, the dewetting velocities in the directions marked **a** and **b** are same and the hole remains circular. After about 5 min of nearly circular growth, the dewetted distance in the **a** direction (the corner direction) still almost linearly increase with the time, but the dewetted distance in the **b** direction (the side-edge direction) slows down substantially. The dewetting kinetics acquires a directional dependence, thus making the hole increasingly noncircular. At a later stage of growth, the velocity of the side edge slightly increases with time because

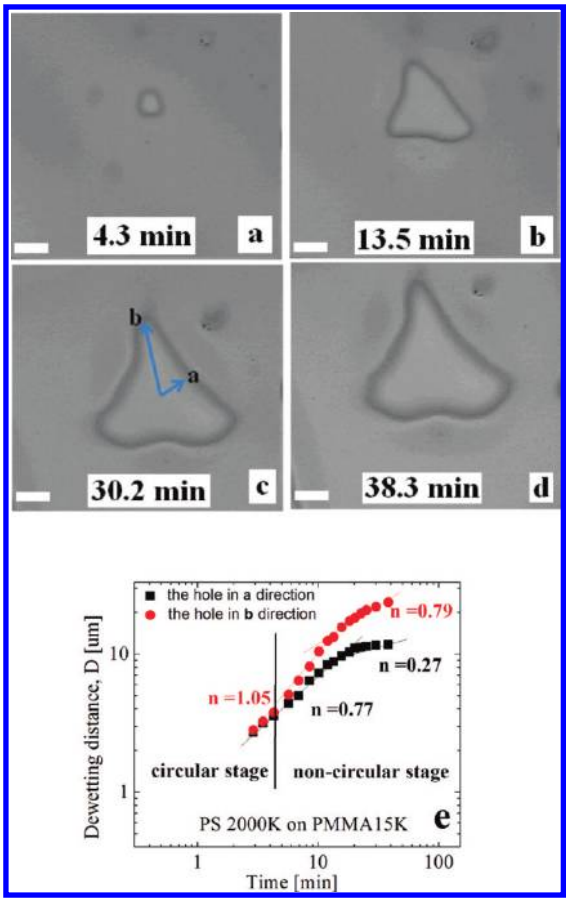

Figure 3. Optical micrographs (a−d) show the morphology of dewetted regions. The bilayer of PS (M_w = 2000 kg/mol, h_U = 42 ± 2 nm) film/the PMMA film (M_w = 15 kg/mol, h_L = 262 nm) was heated at 180 °C. (e) Kinetics of dewetting for a hole. Direction marked **a** denotes the direction of side-edge displacement, whereas **b** shows the direction of corner growth. The size of the bar is 12 μm.

the polymer mass from the dewetted regions is mainly collected in the middle of the side directions. Thus, the faceted side becomes somewhat concave with time.

The AFM images in Figures 4a and 4c show the morphology of the dewetting PS hole rim and the buried PS−PMMA interface, respectively. The latter is imaged after the PS upper layer is removed. Figure 4b shows the profile images of the rim at the location 1, 2, and 3 in Figure 4a, and Figure 4d shows the profile images of the liquid−liquid interface at the location 1′, 2′, and 3′ in Figure 4c. From Figure 4a, we can clearly see that the polymer mass from the dewetted regions is mainly collected in the middle of the side directions but accumulates only slightly in the corner direction. From Figure 4b,d, it is found that the height of the rim at the location of the corner (1 in Figure 4a) is obviously lower than that at other locations (2, 3 in Figure 4a), and the volume of trench at the location of the corner (1′ in Figure 4c) is smaller than that at other locations (2′, 3′ in Figure 4c). These observations imply that the resistance for dewetting at a corner is smaller than that at other locations. Thus, the dewetting velocity along the corner direction is faster than that along the side direction, which leads to anisotropic growth.

The hole growth is a kinetic process in which the most efficient way of growth is by maximizing the driving force and minimizing the resistance. For example, the rim instabilities in the form of

dx.doi.org/10.1021/ma201538p |*Macromolecules* 2011, 44, 9335–9340

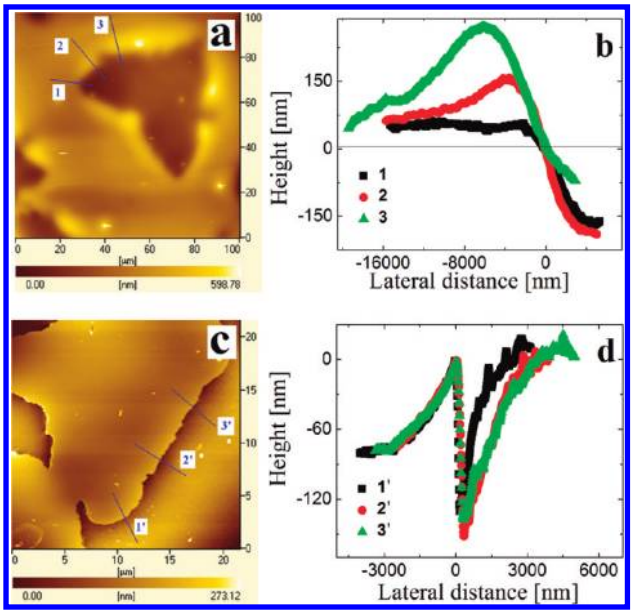

Figure 4. (a) AFM image of the hole-morphology; (b) the profile images of the rim at the location 1, 2, and 3 in (a); (c) the AFM image of the morphology of the liquid−liquid interface after the PS upper layer is removed at the location of the hole; (d) the profile images of the liquid−liquid interface at the location 1′, 2′, and 3′ in (c).

unstable fragmenting fingers can maximize the driving force by increasing the length of the three phase contact line and minimize the resistance force by dissipating the material from the rim into stationary fragmented droplets.[11,34,35,43−45] The latter scenario of auto-optimized fingers also happens in strongly slipping films where a continuous fragmentation of the fingers regulates the rim width to be a low constant, thus making the dewetting velocity to be constant and high. On the low viscosity liquid substrate, we find that the irregular growth of the holes is another efficient dewetting pathway to optimize dewetting by increasing the length of the three-phase contact line and by decreasing the overall resistance by the formation of corners. In the process of the irregular growth, the thick low viscosity liquid substrate plays a key role in producing an almost shear-free liquid−liquid interface engendering a strong slip of the dewetting layer. In the absence of strong slip, the viscous dissipation is dominated by the regions close to the contact line, and the details of the accumulated mass in the rim (height and width) do not control the kinetics. The contact line velocity becomes constant and independent of the rim width.[39] Thus, in the case of no slip, distortions from the circular shape give no kinetic advantage.

When the liquid substrate is thin and viscous, it offers a high resistance and less deformation in the dewetting process owing to the confinement by a solid substrate. The dewetting process on a thin, high M_w viscosity liquid layer is thus similar to on a solid substrate. The viscous dissipation is dominated by the regions close to the contact line regardless of the details of the accumulated mass in its narrow localized rim. The dewetting velocity is low, and the irregular growth is inhibited. An example to this effect is shown by the experiments in Figures 2a and 5, which demonstrates that by increasing the molecular weight of the PMMA, the dewetting slows down and the irregular hole growth is inhibited. Further along this line of reasoning, Figure 6 shows the morphology of PS upper film (M_w = 2000 kg/mol, different film thickness) on the PMMA (M_w = 15 kg/mol, h_L = 262 nm) underlayer. It is seen that the formation of irregular holes is encouraged by a reduction in the PS upper layer thickness. In the case of a thin PS film, the dewetting process becomes fast owing to slippage and the irregular growth is encouraged. However, in the case of the thick PS film, the irregular growth is not seen (Figure 6c).

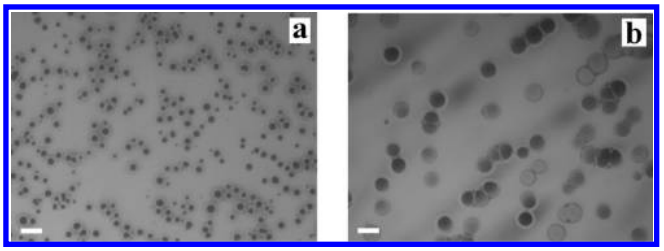

Figure 5. Return of the circular holes on more viscous PMMA substrate layer. The bilayer of PS (M_w = 2000 kg/mol, h_U = 42 ± 2 nm) film/the PMMA film (different M_w, h_L = 262 ± 5 nm) was annealed at 180 °C. (a) M_w = 50 kg/mol, annealing time is 30 min; (b) M_w = 350 kg/mol, annealing time is 150 min. The size of the bar is 20 μm.

This is understood by noting that with strong slippage the influence of a hole in the form of its broad rim extends to far greater distances (>20 μm in Figure 4) than in the case of a nonslipping contact line where its rim is highly narrow and localized (Figure 1a).[36−39] Thus, when several randomly placed holes appear in a slipping film and grow to acquire rims, the film between them becomes nonuniform in height with an irregular, directional distribution of heights as the broad rims of widely separated holes begin to interact. Contrasting Figure 1a for nonslipping films with Figure 2 (for slipping films) shows an uneven direction-dependent distribution of the liquid between the holes in the latter case, whereas the film beyond the narrow rims of nonslipping cases remains uniform. Thus, the resistance to the hole growth also becomes direction dependent, causing faster and slower growth in different directions. In fact, a departure from the circular shape happens also for the nonslipping case, but only when the neighboring rims overlap just before the coalescence. Basically, an early deviation from the circular morphology in slipping films is in this sense similar to the nonslipping films, the difference being in the much greater distances at which the initial holes begin to interact with strong slippage and thus acquire irregular shapes in the early stages of growth. The hole elongation and a faster corner growth can happen along the "channels" of less resistance formed in the uneven film surrounding the holes. From Figure 7, it is seen that the presence of hole 2 obviously influences the shape of hole 1. When the distance between the holes 1 and 2 is about 18 μm, the growth velocity of hole 1 is different in different directions and the hole 1 becomes elongated in the parallel direction of hole 2. The result show that the strong slip has affected the dewetting resistance force in the region between hole 1 and hole 2. Thus, the presence of strong slip in the upper layer is necessary for the morphological optimization of dewetting witnessed in our experiments. The strong slip is favored when the dewetting liquid (substrate liquid) has lower (higher) thickness and a much higher (lower) viscosity, together with entanglement of the polymer chains in the upper dewetting layer. The reason a greatly reduced viscosity in the substrate layer is required to make the dissipation in it comparable to the dewetting layer is owing to its confinement with a solid which causes much higher friction because of the no slip condition at the solid lower layer interface. It is known that the large viscosity ratio of the upper and the lower

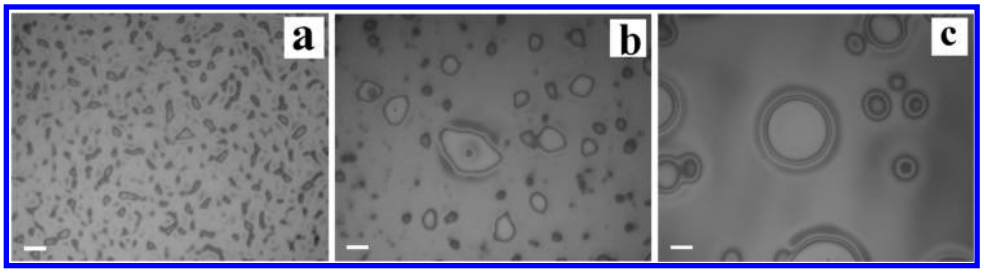

Figure 6. Transition to circular holes with increased thickness of the PS dewetting layer. The bilayer with PS (M_w = 2000 kg/mol, different film thickness h_U) film/the PMMA film (M_w = 15 kg/mol, h_L = 262 nm) was heated at 180 °C. (a) h_U = 18 nm, annealing time is 5 min; (b) h_U = 42 nm, annealing time is 15 min; (c) h_U = 185 nm, annealing time is 40 min. The size of the bar is 20 μm.

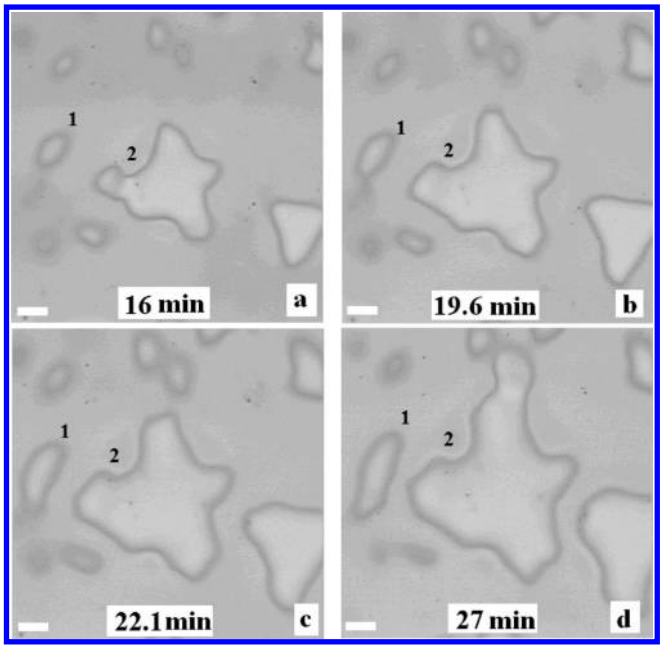

Figure 7. Optical micrographs (a−d) show the morphology at different annealing time. The bilayer of PS (M_w = 2000 kg/mol, h_U = 42 ± 2 nm) film/the PMMA film (M_w = 15 kg/mol, h_L = 262 nm) was heated at 180 °C. The size of the bar is 12 μm.

layers also influences the greater deformation of the underlayer[46] and may thus be correlated to the irregular growth, but may not be the origin of the irregular growth. Further, in addition to low viscous dissipation in the underlayer, slippage may also be greatly promoted by the chain entanglement in the upper layer. To investigate these points, an experiment was performed in which the viscosity ratio was kept high, but the upper layer molecular weight was kept below the entanglement limit. The viscosity of PMMA is far higher than that of PS at the same molecular weight. Thus, a large viscosity ratio of the upper layer and the underlayer could be obtained by using PMMA (10 kg/mol) layer as the upper layer and use PS (2.4 and 4 kg/mol) as the underlayer. The solid substrate used was the Si wafer without the oxide layer. The viscosity ratios for the two molecular weights of PS layers were ~3×10^4 and 5×10^3, respectively. Figure 8 in these cases shows only circular growth of holes, as the strong slip is now suppressed. Thus, we think the origin of the irregular growth is a strong slip of the upper layer, which is engendered by entanglement in the upper layer and aided by the high viscosity ratio and higher thickness of the substrate layer.

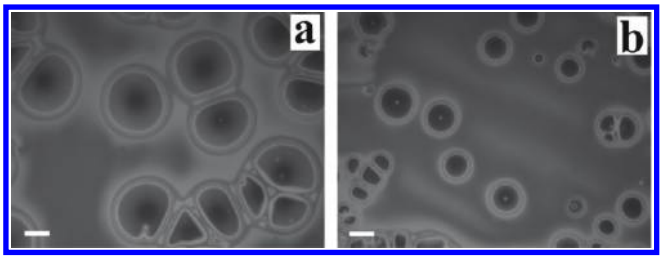

Figure 8. Bilayer of PMMA (M_w = 10 kg/mol, h_U = 38 ± 2 nm) film/the PS film (different M_w, h_L = 200 ± 3 nm)/Si wafer without the oxide layer was annealed at 180 °C. (a) M_w = 2.4 kg/mol, annealing time is 6 s; (b) M_w = 4 kg/mol, annealing time is 6 s. The size of the bar is 20 μm.

As regards the possible role of melt viscoelasticity in irregular growth, we used high annealing temperatures in order to decrease the influence of elasticity. Further, by merely increasing the lower layer thickness and without changing the upper layer molecular weight, the signature of strong slip in the form of anisotropic growth could still be detected. Thus, while viscoelastic behavior of polymer melt could possibly be an important factor, in the experiments reported here, its principal effect seems to be by modifying the slip effect.

All the experimental evidence discussed above together point to the chain entanglement in the dewetting upper layer to be a necessary condition for the irregular growth of holes, but not always sufficient. It appears that entanglement together with a negligible frictional or viscous resistance in the underlayer can induce strong enough slip effects in the upper layer required for anisotropic growth of holes. Such a view is also supported by the fact that irregular hole growth has not been witnessed on solid substrates, notwithstanding slippage induced by entanglement. Thus, a low viscosity thick substrate offering little frictional resistance may be further required to greatly enhance slip.

CONCLUSIONS

We have investigated the kinetics and morphology of holes in dewetting of the unstable upper layer of a thin polymer bilayer (silica−PMMA−PS−air). The relative extent of viscous dissipation in the two layers and the slippage of the dewetting layer on the lower layer are tuned by changing the viscosities and thicknesses and by changing the entanglement of the polymer chains in the upper layer. Strong slippage is engendered when the dewetting layer chains are entangled, and the substrate layer is of low viscosity and high thickness, offering little frictional resistance. In the strong slip cases, we find the growth of holes to be anisotropic, leading to highly irregular and faceted shapes.

Hole growth in a nonslipping film is a highly individualistic process governed entirely by the friction or dissipation in the immediate vicinity of its contact line until the spatially localized and narrow rims of two neighboring holes come in contact. The holes can thus maintain their circular shapes until the onset of the early stages of coalescence. Hole growth in the strongly slipping films, on the other hand, is a cooperative process wherein the long-distance correlations among the holes owing to their very broad rims create a highly nonuniform distribution of film thickness far away from the holes. The local height dependent viscous dissipation is now distributed all along the film. This process creates some preferred, but randomly distributed, directions of growth along which the viscous resistance is less. Regions of higher curvature such as corners appear and grow in the directions of least hindrance. Over time, faceted and irregular structures evolve as a combination of faster moving corners and slower moving straight sides around which more dewetted mass is collected. The irregular growth of holes is thus found to be a new and efficient pathway for auto-optimization of dewetting velocity in strongly slipping films.

AUTHOR INFORMATION

Corresponding Author

*E-mail: ashutos@iitk.ac.in (A.S.), swjoo@yu.ac.kr (S.W.J.). Tel: +82-53-810-2577 or +82-53-810-2568. Fax: +82-53-810-2062.

ACKNOWLEDGMENT

This work is supported by the World Class University Grant R32-2008-000-20082-0 of the National Research Foundation of Korea.

REFERENCES

(1) Brochard-Wyart, F.; J. Daillant, J. *Can. J. Phys.* **1990**, *68*, 1084.
(2) Gabriele, S.; Damman, P.; Sclavons, S.; Desprez, S.; Coppée, S.; Reiter, G.; Hamieh, M.; Akhrass, S. A.; Vilmin, T.; Raphaël, E. *J. Polym. Sci., Part B: Polym. Phys.* **2006**, *44*, 3022.
(3) Reiter, G.; Khanna, R. *Langmuir* **2000**, *16*, 6351.
(4) Reiter, G. *Phys. Rev. Lett.* **1992**, *68*, 75.
(5) Sharma, A.; Reiter, G. *J. Colloid Interface Sci.* **1996**, *178*, 383.
(6) Sharma, A.; Khanna, R. *Phys. Rev. Lett.* **1998**, *81*, 3463.
(7) Brochard-Wyart, F.; Debrégeas, G.; Fondecave, R.; Martin, P. *Macromolecules* **1997**, *30*, 1211.
(8) Damman, P.; Baudelet, N.; Reiter, G. *Phys. Rev. Lett.* **2003** *91*, 216101.
(9) Ziebert, F.; Raphaël, E. *Phys. Rev. E* **2009**, *79*, 031605.
(10) Bäumchen, O.; Jacobs, K. *J. Phys: Condens. Matter* **2010**, *22*, 033102.
(11) Xu, L.; Shi, T. F.; An, L. J. *J. Chem. Phys.* **2008**, *129*, 044904.
(12) Xu, L.; Sharma, A.; Joo, S. W. *Macromolecules* **2010**, *43*, 7759.
(13) Brochard-Wyart, F.; Martin, P.; Redon, C. *Langmuir* **1993** *9*, 3682.
(14) Lambooy, P.; Phelan, K. C.; Haugg, O.; Krausch, G. *Phys. Rev. Lett.* **1996**, *76*, 1110.
(15) Pan, Q.; Winey, K. I.; Hu, H. H.; Composto, R. J. *Langmuir* **1997**, *13*, 1758.
(16) Lin, Z.; Kerle, T.; Russell, T. P.; Schäffer, E.; Steiner, U. *Macromolecules* **2002**, *35*, 3971.
(17) Wang, C.; Krausch, G.; Geoghegan, M. *Langmuir* **2001**, *17*, 6269.
(18) Xu, L.; Reiter, G.; Shi, T. F.; An, L. J. *Langmuir* **2010**, *26*, 7270.
(19) Besancon, B. M.; Green, P. F. *J. Chem. Phys.* **2007**, *126*, 224903.
(20) Xu, L.; Shi, T. F.; An, L. J. *J. Chem. Phys.* **2009**, *130*, 184903.
(21) Al Akhrass, S.; Reiter, G.; Hou, S. Y.; Yang, M. H.; Chang, Y. L.; Chang, F. C.; Wang, C. F.; Yang, A. C-M. *Phys. Rev. Lett.* **2008**, *100*, 178301.
(22) Xu, L.; Yu, X. F.; Shi, T. F.; An, L. J. *Macromolecules* **2008**, *41*, 21.
(23) de Silva, J. P.; Geoghegan, M.; Higgins, A. M.; Krausch, G.; David, M.-O.; Reiter, G. *Phys. Rev. Lett.* **2007**, *98*, 267802.
(24) Fisher, L. S.; Golovin, A. A. *J. Colloid Interface Sci.* **2005**, *291*, 515.
(25) Merabia, S.; Avalos, J. B. *Phys. Rev. Lett.* **2008**, *101*, 208304.
(26) Merkt, D.; Pototsky, A.; Bestehorn, M.; Thiele, U. *Phys. Fluids* **2005**, *17*, 064104.
(27) Pototsky, A.; Bestehorn, M.; Merkt, D.; Thiele, U. *J. Chem. Phys.* **2005**, *122*, 224711.
(28) Pototsky, A.; Bestehorn, M.; Merkt, D.; Thiele, U. *Europhys. Lett.* **2006**, *74*, 665.
(29) Bandyopadhyay, D.; Gulabani, R.; Sharma, A. *Ind. Eng. Chem. Res.* **2005**, *44*, 1259.
(30) Bandyopadhyay, D.; Sharma, A. *J. Chem. Phys.* **2006**, *125*, 054711.
(31) Bandyopadhyay, D.; Sharma, A.; Rastogi, C. *Langmuir* **2008**, *24*, 14048.
(32) Bandyopadhyay, D.; Sharma, A. *J. Phys. Chem. B* **2008**, *112*, 11564.
(33) Bandyopadhyay, D.; Sharma, A. *J. Phys. Chem. C* **2010**, *114*, 2237.
(34) Reiter, G.; Sharma, A. *Phys. Rev. Lett.* **2001**, *87*, 166103.
(35) Gabriele, S.; Coppée, S.; Reiter, G.; Damman, P. *Eur. Phys. J.: Spec. Top.* **2009**, *166*, 55.
(36) Sharma, A. *Eur. Phys. J. E* **2003**, *12*, 397.
(37) Sharma, A.; Kargupta, K. *Appl. Phys. Lett.* **2003**, *83*, 3549.
(38) Kajari, K.; Sharma, A.; Khanna, R. *Langmuir* **2004**, *20*, 244.
(39) Ghatak, A.; Khanna, R.; Sharma, A. *J. Colloid Interface Sci.* **1999**, *212*, 483.
(40) Fox, T. G.; Flory, P. J. *J. Phys. Colloid Chem.* **1951**, *55*, 221.
(41) Fuchs, K.; Friedrich, C.; Weese, J. *Macromolecules* **1996**, *29*, 5893.
(42) Wang, J.-S.; Porter, R. S. *Rheol. Acta* **1995**, *34*, 496.
(43) Reiter, G. *Langmuir* **1993**, *9*, 1344.
(44) Münch, A.; Wagner, B. *Physica D* **2005**, *209*, 178.
(45) Xu, L.; Shi, T. F.; Dutta, P. K.; An, L. J. *J. Chem. Phys.* **2007**, *127*, 144704.
(46) Kostourou, K.; Peschka, D.; Münch, A.; Wagner, B.; Herminghaus, S.; Seemann, R. *Chem. Eng. Process.* **2011**, *50*, 531.